

## RESEARCH ARTICLE

View Article Online  
View Journal | View IssueCite this: *Org. Chem. Front.*, 2025,  
12, 2732Photoelectrochemical iron–cobalt synergistic  
catalysis for C(sp<sup>3</sup>)–H alkenylation†Jia-Lin Tu, <sup>a</sup> Ao-Men Hu,<sup>a</sup> Chao Yang, <sup>a</sup> Lin Guo\*<sup>a</sup> and Wujiong Xia \*<sup>a,b</sup>

Electrocatalysis and photocatalysis have both emerged as increasingly feasible platforms in sustainable synthesis. This study explores a novel photoelectrochemical synergistic strategy, achieving non-directed C(sp<sup>3</sup>)–H alkenylation reaction utilizing an iron–cobalt dual catalytic system. With the synergy of photoelectrochemical redox catalysis and iron–cobalt catalysis, efficient C(sp<sup>3</sup>)–H alkenylation reaction of alkanes as well as dehydrogenation occur without the need for chemical oxidants or reductants, yielding hydrogen gas as the sole byproduct. The electric current is employed to modulate the oxidation states of the catalysts, fulfilling a role similar to that of external oxidants typically used in transition metal catalysis. This method demonstrates unconventional regioselectivity, with a preference for alkenylation at the 1° C–H bonds. This research not only demonstrates that alkenes as radical acceptors can influence the regioselectivity but also offers a promising pathway for advancing iron-catalyzed C–H functionalization.

Received 2nd January 2025,  
Accepted 21st February 2025

DOI: 10.1039/d5qo00017c

rsc.li/frontiers-organic

## Introduction

Alkane resources are abundant and cost-effective, widely present in natural gas and associated with petroleum. However, despite their abundant reserves, only a small portion is converted into high-value chemical products. It is crucial to sensibly utilize fossil resources such as petroleum and natural gas.<sup>1</sup> The functionalization of inert alkanes poses a significant challenge due to the high bond energy of C–H bonds.<sup>2</sup> To achieve meaningful transformations, an increasing variety of hydrogen abstractors have been developed, including eosin Y,<sup>3</sup> diaryl ketones,<sup>4</sup> and decatungstate.<sup>5</sup> Recent years have witnessed remarkable advancements in transition metal-catalyzed reactions leveraging visible light irradiation.<sup>6</sup> Cost-effective transition metals such as iron and copper, employing chlorine radicals produced *via* the photoinduced ligand-to-metal charge transfer (LMCT) process, have gained substantial attention as potent hydrogen atom transfer (HAT) agents in current research.<sup>7</sup> The development of these radical-mediated C–H functionalization reactions represents a substantial advancement in the formation of diverse chemical bonds.<sup>8</sup> However, a crucial point in the discussion of carbon–hydrogen activation revolves around the regioselectivity of hydrogen atom transfer.

Apart from the diverse range and bulkiness of HAT species,<sup>9</sup> we propose that the use of radical acceptors plays a key role in influencing reaction selectivity.<sup>8a,10</sup> Taking 2,3-dimethylbutane as an example, the bond dissociation energy of 1° C(sp<sup>3</sup>)–H bonds significantly exceeds that at 3° C(sp<sup>3</sup>)–H bonds, implying a higher reactivity at the tertiary C(sp<sup>3</sup>)–H bonds.<sup>2b</sup> Surprisingly, in Duan's and our investigations of photoinduced iron-catalyzed C(sp<sup>3</sup>)–H borylation,<sup>8a</sup> thiolation,<sup>8a,b</sup> sulfonylation,<sup>8a,b</sup> phosphorylation<sup>8c</sup> and alkynylation reactions,<sup>8i</sup> the reaction sites predominantly showed 1° C–H selectivity, with no observation of C(sp<sup>3</sup>)–H functionalization at the weak 3° C–H bonds (Scheme 1a).

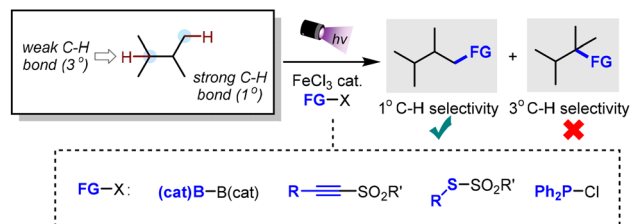
To explore how other radical acceptors affect the regioselectivity of the C(sp<sup>3</sup>)–H functionalization reactions, our attention turned towards iron photocatalytic C(sp<sup>3</sup>)–H alkenylation. This shift arose from the potential of olefins in organic synthesis due to their remarkably diverse chemical reactivity encompassing addition and oxidation reactions. Thus, achieving direct alkenylation of simple alkanes holds significant synthetic potential in constructing and deriving complex molecules.<sup>11</sup> Iron and cobalt exhibit similar chemical properties and reactivity (Scheme 1b).<sup>12</sup> Due to the potential mutual interference in the redox processes of iron and cobalt catalysts within the reaction system, the exploration of their synergistic catalytic effects under photochemical conditions remains relatively limited in the current literature.<sup>13</sup> Electrocatalysis and photocatalysis have emerged as increasingly feasible platforms for sustainable molecular assembly by synergistically integrating electrochemical synthesis and photochemical oxidation–reduction catalysis within a single system. This approach eliminates the need for external chemical oxidants and reductants,

<sup>a</sup>State Key Lab of Urban Water Resource and Environment, School of Science, Harbin Institute of Technology (Shenzhen), Shenzhen, 518055, China.

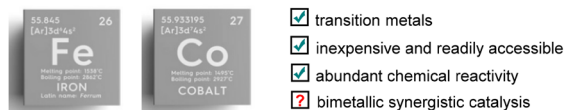
E-mail: guolin@hit.edu.cn, xiawj@hit.edu.cn

<sup>b</sup>School of Chemistry and Chemical Engineering, Henan Normal University, Xinxiang, Henan 453007, China† Electronic supplementary information (ESI) available. See DOI: <https://doi.org/10.1039/d5qo00017c>

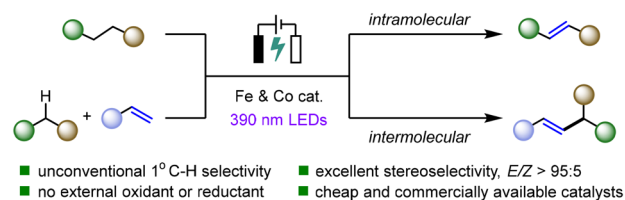
## a) Regioselectivity of C-H functionalization influenced by radical acceptors



## b) Similarities between metallic iron and cobalt



## c) Photoelectrocatalytic alkane-to-alkene conversion by iron-cobalt synergy (this work)



Scheme 1 C-H functionalization reactions via iron photocatalysis.

as the electric current serves as a clean electron source and sink to modulate the redox states of the catalysts.<sup>14</sup> Building on previous seminal work<sup>8,14</sup> and the superiority of the photoelectrocatalytic framework,<sup>15</sup> we envision exploring an innovative and sustainable platform for non-directed C(sp<sup>3</sup>)-H functionalization employing iron-cobalt bimetallic catalysis. In our proposed strategy, the chlorine radicals formed under iron-induced light act as HAT species, while the generated Fe<sup>2+</sup> undergoes oxidation at the anode.<sup>5m</sup> On the other hand, owing to its higher oxidation potential, Co<sup>3+</sup> acts as a cathodic catalyst, enabling separate catalytic cycles for iron and cobalt at the anode and cathode, respectively, thereby preventing competitive reactions at the anode.<sup>16</sup>

Herein, we report the successful realization of a photoelectrically synergistic induced iron/cobalt dual catalysis, enabling the non-directed C(sp<sup>3</sup>)-H alkenylation reaction (Scheme 1c). Our C-H alkenylation protocol is applicable not only to simple alkanes and silanes but also to various ketones and nitriles. Furthermore, this photoelectric strategy appears to have a preference for stronger 1° C-H bonds, suggesting that alkenes, when used as radical acceptors, could potentially influence the selectivity of HAT.

## Results and discussion

In the initial phase of our research, we selected cyclohexane **1** and styrene **2** as model substrates for condition optimization, with detailed experimental conditions outlined in Table 1. Graphite felt (GF) was employed as the anode, and graphite rod as the cathode, with the addition of FeCl<sub>3</sub>, Co(OTf)<sub>2</sub>, di-

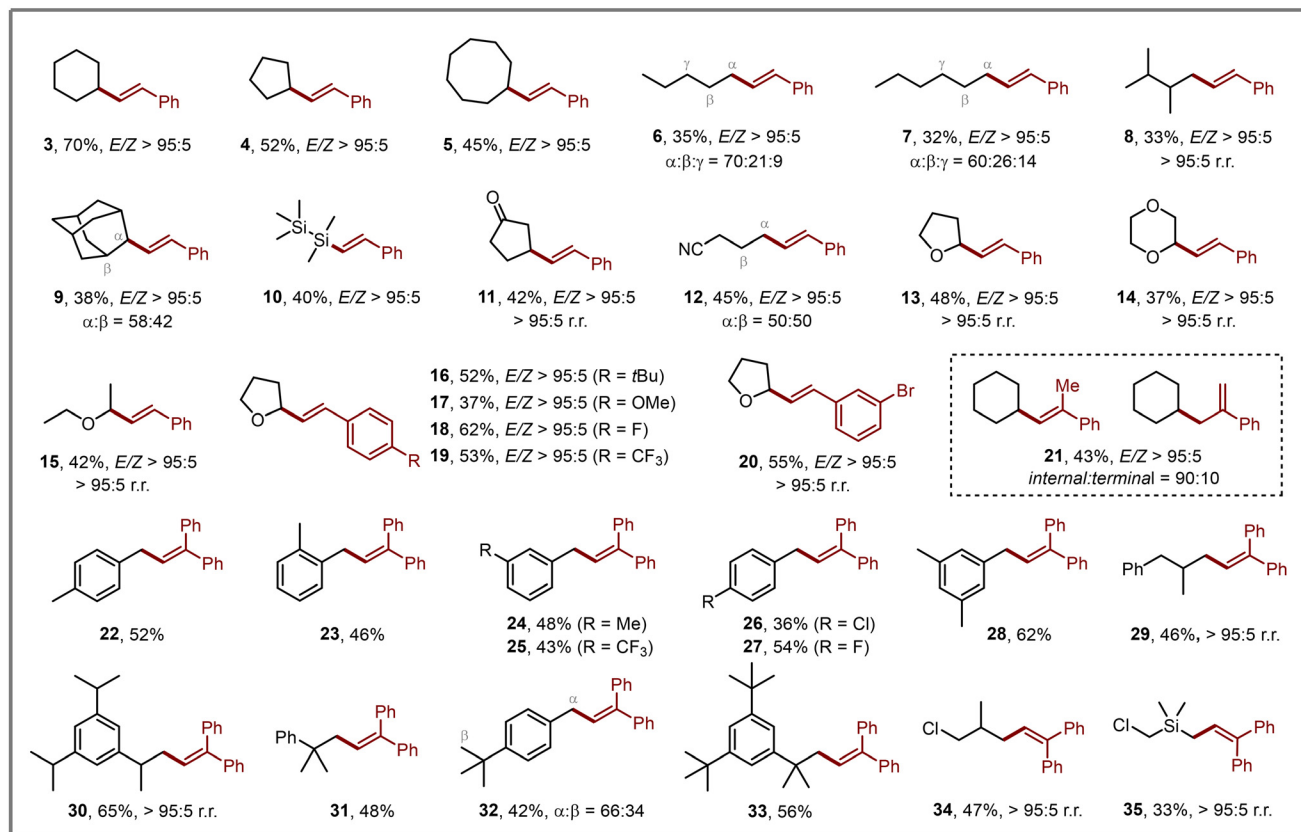
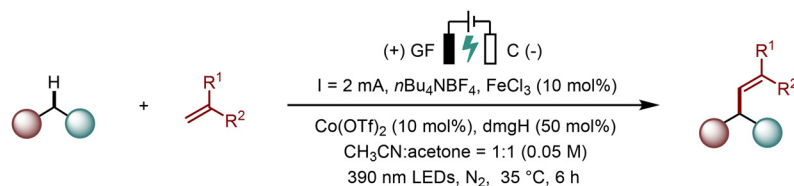
Table 1 Optimization studies<sup>a</sup>

Entry	Deviation from standard conditions	3 <sup>b</sup> (%)
1	None	70
2	<i>n</i> Bu <sub>4</sub> NCl instead of <i>n</i> Bu <sub>4</sub> NBF <sub>4</sub>	38
3	<i>n</i> Bu <sub>4</sub> NPF <sub>6</sub> instead of <i>n</i> Bu <sub>4</sub> NBF <sub>4</sub>	35
4	Al plate as cathode	42
5	Ni plate as cathode	47
6	CuCl <sub>2</sub> instead of FeCl <sub>3</sub>	<5
7	Co(acac) <sub>2</sub> instead of Co(OTf) <sub>2</sub>	45
8	CoSO <sub>4</sub> instead of Co(OTf) <sub>2</sub>	65
9	<i>I</i> = 5 mA	60
10	CH <sub>3</sub> CN as solvent	40
11	Acetone as solvent	Trace
12	w/o dmgH, FeCl <sub>3</sub> or Co(OTf) <sub>2</sub>	N.D.
13	w/o electricity or light	Trace

<sup>a</sup> Reaction conditions: **1** (2.0 mmol, 10.0 equiv.), **2** (0.20 mmol, 1.0 equiv.), FeCl<sub>3</sub> (10 mol%), Co(OTf)<sub>2</sub> (10 mol%), dmgH (50 mol%), *n*Bu<sub>4</sub>NBF<sub>4</sub> (2.0 equiv.), *I* = 2.0 mA, 6 h, CH<sub>3</sub>CN : acetone = 1 : 1 (4.0 ml), 35 °C, 390 nm LEDs (18 W), graphite felt (GF) as anode, graphite rod as cathode, undivided cell. <sup>b</sup> Yields are of isolated products after chromatographic purification. dmgH: dimethylglyoxime. N.D.: not detected.

methylglyoxime (dmgH), and tetrabutylammonium tetrafluoroborate (*n*Bu<sub>4</sub>NBF<sub>4</sub>) into the reaction system. Acetone:acetonitrile (v/v = 1:1) was used as solvent. Under nitrogen conditions, the reaction between **1** and **2** proceeded efficiently with a constant current of 2 mA, achieving an intermolecular C(sp<sup>3</sup>)-H olefination reaction and yielding product **3** in 70% yield with exclusive *E*-selectivity (Table 1, entry 1). Subsequently, we tested several alternative electrolytes such as *n*Bu<sub>4</sub>NCl and *n*Bu<sub>4</sub>NPF<sub>6</sub>, but unsatisfactory results were obtained (entries 2 and 3). Substituting the carbon felt anode with an aluminum rod or nickel sheet led to a significant decrease in the yield (entries 4 and 5). When copper chloride was used instead of iron chloride, the reaction scarcely proceeded (entry 6). The use of Co(acac)<sub>2</sub> and CoSO<sub>4</sub> as cobalt catalysts resulted in varying degrees of yield reduction (entries 7 and 8). Additionally, adjusting the operating current to 5 mA led to a slight decrease in the yield of alkylation products (entry 9). Furthermore, the reaction was subjected to solvent screening, revealing a drastic drop in yield to 40% when acetonitrile was used (entry 10), while trace of target product was detected with the use of acetone as solvent (entry 11). In the absence of dmgH, iron or cobalt catalyst, the reaction did not occur. Lack of electric current or light also prevented the reaction from proceeding, underscoring the crucial role of both electric current and light in this transformation (entries 12 and 13).

Upon establishing the optimal conditions, we initiated the substrate expansion for this photoinduced C(sp<sup>3</sup>)-H olefina-



**Scheme 2** Substrate scope of  $\text{C}(\text{sp}^3)\text{-H}$  alkenylation reaction. Reaction conditions: hydrocarbon substrate (2.0 mmol, 10.0 equiv.), alkene substrate (0.20 mmol, 1.0 equiv.),  $\text{FeCl}_3$  (10 mol%),  $\text{Co}(\text{OTf})_2$  (10 mol%),  $\text{dmgH}$  (50 mol%),  $n\text{Bu}_4\text{NBF}_4$  (2.0 equiv.),  $I = 2.0$  mA, 6 h,  $\text{CH}_3\text{CN}:\text{acetone} = 1:1$  (4.0 ml), 35 °C, 390 nm LEDs (18 W), graphite felt (GF) as anode, graphite rod as cathode, undivided cell. Yields are of isolated products after chromatographic purification.

tion, systematically exploring a range of alkane and alkene derivatives (Scheme 2). Using styrene as the template substrate, we tested various alkanes. Gratifyingly, commonly used alkanes, silanes, ketones, nitriles, ethers, and others proved compatible with our photoredox system, delivering the desired products in acceptable yields with exclusive  $E$ -selectivity (3–15). For linear alkanes such as  $n$ -pentane,  $n$ -hexane, and 2,3-dimethylbutane,  $\text{C}(\text{sp}^3)\text{-H}$  alkenylation exhibited multiple reaction sites, yet the reaction predominantly occurred at the terminal methyl position. This terminal regioselectivity closely resembled previous reports, suggesting that alkenes as radical acceptors also influence reaction selectivity (6–8). In the case of adamantane, the reaction favored the less sterically hindered methylene positions (9). For the reaction of silanes, the reaction afforded the corresponding olefination products in reasonable yields (10). Furthermore, both cyclopentanone and butyronitrile underwent  $\text{C}(\text{sp}^3)\text{-H}$  olefination smoothly, demonstrating excellent functional group compatibility of the

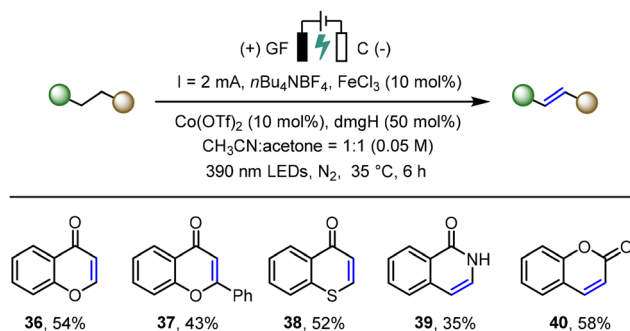
reaction (11–12). The observed regioselectivity is likely determined by the steric properties of both the HAT reagent and the radical acceptor. Next, we directed our attention towards the modification of ether compounds. The use of tetrahydrofuran, 1,4-dioxane, and ethyl ether all provided the desired products in moderate yields and excellent  $E/Z$  ratios (13–15). Additionally, using tetrahydrofuran as the model substrate, we expanded our investigation for the scope of alkenes. The results revealed that the reaction proceeded well regardless of whether styrenes bear electron-donating substituents on the aromatic rings such as  $tert$ -butyl and methoxy groups, or electron-withdrawing substituents such as halogens and trifluoromethyl groups (16–20). For  $\alpha$ -methylstyrene as the alkenylic acceptor, the reaction with cyclohexane as the substrate presents two possible elimination pathways – olefin formation at the internal position and at the terminus. The reaction proceeded in 43% yield with a selectivity of 9:1 (internal:terminal) (21). Finally, we sought to test whether toluene

derivatives could serve as suitable alkyl substrates for the reaction. Unfortunately, when styrene was used as the olefin substrate, the reaction product had very similar polarity with the excess alkane substrate, making the isolation of pure products very challenging. Therefore, we opted to expand this part of the substrate scope by employing 1,1-diphenylethylene as the model substrate. The photoelectrochemical reaction of commonly used solvents such as *p*-xylene, *o*-xylene, and *m*-xylene afforded the corresponding alkene products in moderate yields (22–24). Toluene derivatives bearing trifluoromethyl groups or halogens on the aromatics underwent the photoelectrochemical reactions well to give products 25–27 in acceptable yields with exclusive *E*-selectivity. When 1,3,5-triisopropylbenzene participated in the reaction, regioselectivity of terminal methyl group was exclusively achieved (30). Similarly, *tert*-butylbenzene reacted to give product 31 as expected, while 4-methyl-*tert*-butylbenzene containing two reactive C(sp<sup>3</sup>)–H sites predominantly underwent the reaction at the benzylic methyl group (32). 1,3,5-Tri-*tert*-butylbenzene also proceeded smoothly, yielding the corresponding alkene products (33). Furthermore, for chlorinated alkanes, the reaction worked well to afford the desired products in acceptable yields (34–35), which further demonstrated the generality of this reaction.

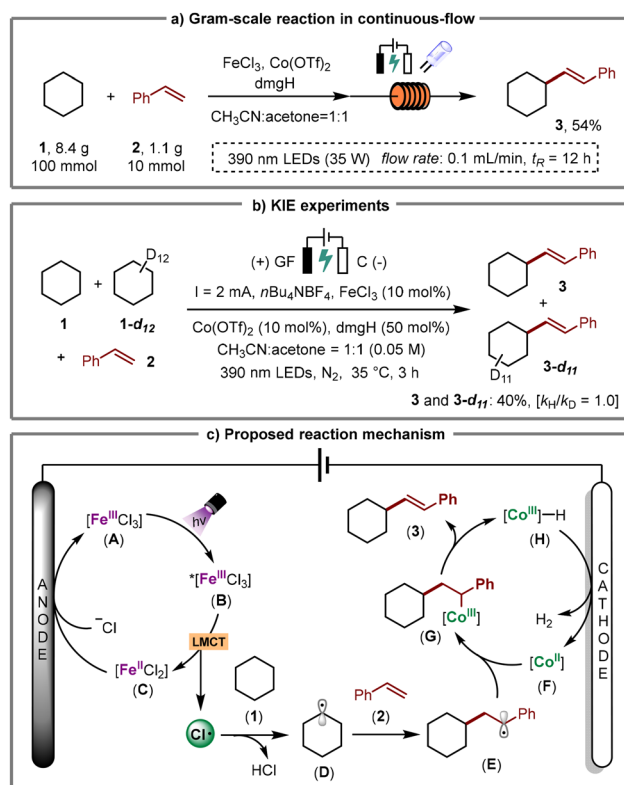
To delve into the capabilities of this photoelectrochemical strategy, we next successfully expanded its application to intramolecular dehydrogenation reactions *via* radical-mediated  $\alpha$ -hydrogen ( $\alpha$ -H) elimination process of various heteroatoms. As illustrated in Scheme 3, a series of dehydrogenation products could be achieved, encompassing compounds containing  $\alpha$ -hydrogen of oxygen, sulfur, and nitrogen atoms (36–40).

To further showcase the synthetic potential of the iron/cobalt-photoinduced ligand-to-metal charge transfer (LMCT) method, we conducted a gram-scale continuous-flow reaction using cyclohexane (1) and styrene (2) as substrates, as depicted in Scheme 4a. By applying a flow rate of 0.1 mL min<sup>-1</sup> and a reaction time of 12 hours, we were able to scale up the C(sp<sup>3</sup>)–H alkenylation reaction by 50-fold. The reaction solution, upon purification, yielded the corresponding alkenylated product (3) in a 54% yield.

In order to gain deeper insights into the reaction mechanism, a series of mechanistic experiments were conducted (further details can be found in the ESI†). Kinetic isotope effect (KIE) experiments were conducted to probe whether



**Scheme 3** Dehydrogenation reactions *via* iron & cobalt photocatalysis.



**Scheme 4** Gram-scale reaction in continuous flow and mechanistic studies.

hydrogen atom transfer (HAT) serves as the rate-determining step in the overall reaction mechanism. The reaction of styrene with equimolar amounts of cyclohexane and deuterated cyclohexane under standard conditions of C–H alkenylation for 3 hours yielded a mixture of 3 and isotopically labeled 3-*d*<sub>11</sub> in 40% yield, with secondary kinetic isotope effects ( $k_H/k_D = 1.0$ ), indicating that the hydrogen/deuterium atom abstraction step is not the turnover-limiting step in the iron/cobalt catalytic cycle (Scheme 4b).

Based on the aforementioned experimental results and literature survey,<sup>8,17</sup> a plausible mechanism for the iron/cobalt synergistic catalyzed C(sp<sup>3</sup>)–H alkenylation reaction is proposed, as depicted in Scheme 4c. The process initiates with ligand-to-metal charge transfer from the excited state FeCl<sub>3</sub> catalyst (B), generating an electrophilic chlorine radical. This chlorine radical abstracts a hydrogen atom from cyclohexane (1), producing a reactive alkyl radical (D), while Fe(II) is oxidized to Fe(III) at the anode. Simultaneously, the formed alkyl radical undergoes addition to the alkene (2), generating an additional radical intermediate (E), which is subsequently captured by a Co(II) complex to form an organocobalt(III) complex (G). The crucial  $\beta$ -H elimination step readily occurs, yielding alkene compound (3) and a Co(III)–H intermediate (H). The reaction of the Co(III)–H complex with a proton leads to H<sub>2</sub> extrusion, followed by electrochemical reduction of the Co(III) complex at the cathode to regenerate the Co(II) complex, thus renewing the cobalt catalyst.

## Conclusions

In summary, we describe an unprecedented photoelectrochemical synergistic strategy for the non-directed C(sp<sup>3</sup>)-H alkenylation of inert alkanes using an iron-cobalt bimetallic catalytic system. Through the photo-induced ligand-to-metal charge transfer (LMCT) process and the electrochemical anodic oxidation coupled with cathodic reduction, combined with the synergistic catalysis of iron & cobalt, we have achieved research on the C(sp<sup>3</sup>)-H alkenylation of unactivated alkanes. Experimental results indicate that alkenes, serving as radical acceptors, can also influence the regioselectivity of hydrogen atom transfer (HAT), with the observed preference for alkenylation at primary C-H bonds likely being determined by the steric properties of both the HAT reagent and the radical acceptor.

## Data availability

Data for this article, including the ESI† are available at Organic Chemistry Frontiers at <https://doi.org/10.1039/D5QO00017C>. The data supporting this article have been included as part of the ESI.†

## Conflicts of interest

There are no conflicts to declare.

## Acknowledgements

We are grateful for the financial support from the National Natural Science Foundation of China (No. 22101066, 22471049), the Science and Technology Plan of Shenzhen (No. JCYJ20210324133001004, JCYJ20220531095016036, JCYJ20230807094408017, and GXWD20220817131550002), the Natural Science Foundation of Guangdong (No. 2022A1515010863), and Guangdong Basic and Applied Basic Research Foundation (No. 2021A1515220069). W. X. is grateful for the Talent Recruitment Project of Guangdong (No. 2019QN01L753). The project was also supported by State Key Laboratory of Urban Water Resource and Environment (Harbin Institute of Technology) (No. 2022TS23) and the Open Research Fund of the School of Chemistry and Chemical Engineering, Henan Normal University.

## References

- (a) C. Wang, F. Liu and Z. Shi, Homogeneous functionalization of light alkanes, *Sci. Sin.: Chim.*, 2020, **50**, 756–765; (b) F. D. Mango, The origin of light cycloalkanes in petroleum, *Geochim. Cosmochim. Acta*, 1990, **54**, 23–27.
- (a) H. Cao, X. Tang, H. Tang, Y. Yuan and J. Wu, Photoinduced intermolecular hydrogen atom transfer reactions in organic synthesis, *Chem. Catal.*, 2021, **1**, 523; (b) L. Capaldo, D. Ravelli and M. Fagnoni, Direct Photocatalyzed Hydrogen Atom Transfer (HAT) for Aliphatic C-H Bonds Elaboration, *Chem. Rev.*, 2022, **122**, 1875–1924; (c) H. Yi, G. Zhang, H. Wang, Z. Huang, J. Wang, A. K. Singh and A. Lei, Recent Advances in Radical C-H Activation/Radical Cross-Coupling, *Chem. Rev.*, 2017, **117**, 9016–9085; (d) A. Ghosh, P. Pyne, S. Ghosh, D. Ghosh, S. Majumder and A. Hajra, Visible-light-induced metal-free coupling of C(sp<sup>3</sup>)-H sources with heteroarenes, *Green Chem.*, 2022, **24**, 3056–3080.
- (a) D.-M. Yan, J.-R. Chen and W.-J. Xiao, New Roles for Photoexcited Eosin Y in Photochemical Reactions, *Angew. Chem., Int. Ed.*, 2019, **58**, 378; (b) H. Cao, D. Kong, L.-C. Yang, S. Chanmungkalakul, T. Liu, J. L. Piper, Z. Peng, L. Gao, X. Liu, X. Hong and J. Wu, Brønsted acid-enhanced direct hydrogen atom transfer photocatalysis for selective functionalization of unactivated C(sp<sup>3</sup>)-H bonds, *Nat. Synth.*, 2022, **1**, 794; (c) J. Dey, S. Paul, M. Bhakat and J. Guin, *Org. Lett.*, 2022, **24**, 8047–8051; (d) J. Yan, H. Tang, E. J. R. Kuek, X. Shi, C. Liu, M. Zhang, J. L. Piper, S. Duan and J. Wu, Divergent functionalization of aldehydes photocatalyzed by neutral eosin Y with sulfone reagents, *Nat. Commun.*, 2021, **12**, 7214; (e) S. P. Singh, V. Srivastava, P. K. Singh and P. P. Singh, Visible-light induced eosin Y catalysed C(sp<sup>2</sup>)-H alkylation of carbonyl substrates via direct HAT, *Tetrahedron*, 2023, **132**, 133245.
- (a) M.-J. Zhou, L. Zhang, G. Liu, C. Xu and Z. Huang, Site-Selective Acceptorless Dehydrogenation of Aliphatics Enabled by Organophotoredox/Cobalt Dual Catalysis, *J. Am. Chem. Soc.*, 2021, **143**, 16470; (b) T. Hoshikawa and M. Inoue, Photoinduced direct 4-pyridination of C(sp<sup>3</sup>)-H Bonds, *Chem. Sci.*, 2013, **4**, 3118; (c) B. Abadie, D. Jardel, G. Pozzi, P. Toullec and J.-M. Vincent, Dual Benzophenone/Copper-Photocatalyzed Giese-Type Alkylation of C(sp<sup>3</sup>)-H Bonds, *Chem. - Eur. J.*, 2019, **25**, 16120–16127; (d) M.-J. Zhou, L. Zhang, G. Liu, C. Xu and Z. Huang, Site-Selective Acceptorless Dehydrogenation of Aliphatics Enabled by Organophotoredox/Cobalt Dual Catalysis, *J. Am. Chem. Soc.*, 2021, **143**, 16470–16485; (e) S. Kamijo, M. Hirota, K. Tao, M. Watanabe and T. Murafuji, Photoinduced sulfonylation of cyclic ethers, *Tetrahedron Lett.*, 2014, **55**, 5551–5554.
- (a) X. Y. Yuan, G. P. Yang and B. Yu, Photoinduced Decatungstate-Catalyzed C-H Functionalization, *Chin. J. Org. Chem.*, 2020, **40**, 3620; (b) H. Cao, Y. Kuang, X. Shi, K. L. Wong, B. B. Tan, J. M. C. Kwan, X. Liu and J. Wu, Photoinduced site-selective alkenylation of alkanes and aldehydes with aryl alkenes, *Nat. Commun.*, 2020, **11**, 1956; (c) J. G. West, D. Huang and E. J. Sorensen, Acceptorless dehydrogenation of small molecules through cooperative base metal catalysis, *Nat. Commun.*, 2015, **6**, 10093; (d) Q. Wang, S. Ni, X. Wang, Y. Wang and Y. Pan, Visible-light-mediated tungsten-catalyzed C-H amination of unactivated alkanes with nitroarenes, *Sci. China: Chem.*, 2022, **65**, 678–685.

- 6 (a) L. H. M. de Groot, A. Ilic, J. Schwarz and K. Wärnmark, *J. Am. Chem. Soc.*, 2023, **145**, 9369–9388; (b) W.-J. Zhou, X.-D. Wu, M. Miao, Z.-H. Wang, L. Chen, S.-Y. Shan, G.-M. Cao and D.-G. Yu, Light Runs Across Iron Catalysts in Organic Transformations, *Chem. – Eur. J.*, 2020, **26**, 15052–15064; (c) A. Reichle and O. Reiser, Light-induced homolysis of copper(II)-complexes – a perspective for photocatalysis, *Chem. Sci.*, 2023, **14**, 4449–4462.
- 7 (a) Y. Abderrazak, A. Bhattacharyya and O. Reiser, Visible-Light-Induced Homolysis of Earth-Abundant Metal-Substrate Complexes: A Complementary Activation Strategy in Photoredox Catalysis, *Angew. Chem., Int. Ed.*, 2021, **60**, 21100; (b) F. Juliá, Ligand-to-Metal Charge Transfer (LMCT) Photochemistry at 3d-Metal Complexes: An Emerging Tool for Sustainable Organic Synthesis, *ChemCatChem*, 2022, **14**, e202200916; (c) F. Glaser, A. Aydogan, B. Elias and L. Troian-Gautier, The great strides of iron photosensitizers for contemporary organic photoredox catalysis: On our way to the holy grail?, *Coord. Chem. Rev.*, 2024, **500**, 215522.
- 8 (a) J.-L. Tu, A.-M. Hu, L. Guo and W. Xia, Iron-Catalyzed C(sp<sup>3</sup>)-H Borylation, Thiolation, and Sulfinylation Enabled by Photoinduced Ligand-to-Metal Charge Transfer, *J. Am. Chem. Soc.*, 2023, **145**, 7600; (b) A.-M. Hu, J.-L. Tu, M. Luo, C. Yang, L. Guo and W. Xia, An iron-catalyzed C–S bond-forming reaction of carboxylic acids and hydrocarbons via photo-induced ligand to metal charge transfer, *Org. Chem. Front.*, 2023, **10**, 4764–4773; (c) W. Shi, P.-F. Zhong, X.-K. Qi, C. Yang, L. Guo and W. Xia, Photoinduced ligand-to-iron charge transfer enabled C(sp<sup>3</sup>)-H phosphorylation of hydrocarbons, *Green Chem.*, 2023, **25**, 7817–7824; (d) S. M. Treacy and T. Rovis, Copper Catalyzed C(sp<sup>3</sup>)-H Bond Alkylation via Photoinduced Ligand-to-Metal Charge Transfer, *J. Am. Chem. Soc.*, 2021, **143**, 2729–2735; (e) Y. Jin, Q. Zhang, L. Wang, X. Wang, C. Meng and C. Duan, Convenient C(sp<sup>3</sup>)-H bond functionalisation of light alkanes and other compounds by iron photocatalysis, *Green Chem.*, 2021, **23**, 6984–6989; (f) N. Xiong, Y. Dong, B. Xu, Y. Li and R. Zeng, Mild Amide Synthesis Using Nitrobenzene under Neutral Conditions, *Org. Lett.*, 2022, **24**, 4766–4771; W. Fang, H.-Q. Wang, W. Zhou, Z.-W. Luo and J.-J. Dai, Photoinduced C(sp<sup>3</sup>)-H borylation of alkanes mediated by copper(II) chloride, *Chem. Commun.*, 2023, **59**, 7108–7111; (g) Z.-T. Pan, L.-M. Shen, F. W. Dagnaw, J.-J. Zhong, J.-X. Jian and Q.-X. Tong, Minisci reaction of heteroarenes and unactivated C(sp<sup>3</sup>)-H alkanes via a photo-generated chlorine radical, *Chem. Commun.*, 2023, **59**, 1637–1640; (h) Z.-Y. Dai, S.-Q. Zhang, X. Hong, P.-S. Wang and L.-Z. Gong, A practical FeCl<sub>3</sub>/HCl photocatalyst for versatile aliphatic C–H functionalization, *Chem Catal.*, 2022, **2**, 1211–1222; (i) Y. Jin, L. Wang, Q. Zhang, Y. Zhang, Q. Liao and C. Duan, Photo-induced direct alkynylation of methane and other light alkanes by iron catalysis, *Green Chem.*, 2021, **23**, 9406–9411; (j) A. Chinchole, M. A. Henriquez, D. Cortes-Arriagada, A. R. Cabrera and O. Reiser, Iron(III)-Light-Induced Homolysis: A Dual Photocatalytic Approach for the Hydroacylation of Alkenes Using Acyl Radicals via Direct HAT from Aldehydes, *ACS Catal.*, 2022, **12**, 13549–13554; (k) Q. Zhang, S. Liu, J. Lei, Y. Zhang, C. Meng, C. Duan and Y. Jin, Iron-Catalyzed Photoredox Functionalization of Methane and Heavier Gaseous Alkanes: Scope, Kinetics, and Computational Studies, *Org. Lett.*, 2022, **24**, 1901–1906; (l) L. Zou, X. Wang, S. Xiang, W. Zheng and Q. Lu, Paired Oxidative and Reductive Catalysis: Breaking the Potential Barrier of Electrochemical C(sp<sup>3</sup>)-H Alkenylation, *Angew. Chem., Int. Ed.*, 2023, **62**, e202301026; (m) W. Wei, S. L. Homölle, T. von Münchow, Y. Li, I. Maksso and L. Ackermann, Photoelectrochemical Si–H and Ge–H activation by iron catalysis, *Cell Rep. Phys. Sci.*, 2023, **4**, 101550; (n) P. Li, J.-L. Tu, H. Gao, C. Shi, Y. Zhu, L. Guo, C. Yang and W. Xia, FeCl<sub>3</sub>-Catalyzed C(sp<sup>3</sup>)-H Heteroarylation Enabled by Photoinduced Ligand-to-Metal Charge Transfer, *Adv. Synth. Catal.*, 2024, **366**, 220–224; (o) D. I. Ioannou, L. Capaldo, J. Sanramat, J. N. H. Reek and T. Noël, Accelerated Electrophotocatalytic C(sp<sup>3</sup>)-H Heteroarylation Enabled by an Efficient Continuous-Flow Reactor, *Angew. Chem., Int. Ed.*, 2023, **62**, e202315881; (p) H. Liu, K. Wang, S. Ye, Q. Zhu and H. Huang, Iron-catalyzed C(sp<sup>3</sup>)-H phosphorylation via photoinduced LMCT, *Org. Chem. Front.*, 2024, **11**, 2027–2032.
- 9 (a) G. S. Lee, J. Won, S. Choi, M.-H. Baik and S. H. Hong, Synergistic Activation of Amides and Hydrocarbons for Direct C(sp<sup>3</sup>)-H Acylation Enabled by Metallaphotoredox Catalysis, *Angew. Chem., Int. Ed.*, 2020, **59**, 16933–16942; (b) G. S. Lee, B. Park and S. H. Hong, Stereoretentive cross-coupling of chiral amino acid chlorides and hydrocarbons through mechanistically controlled Ni/Ir photoredox catalysis, *Nat. Commun.*, 2022, **13**, 5200; (c) P. Jia, Q. Li, W. C. Poh, H. Jiang, H. Liu, H. Deng and J. Wu, Light-Promoted Bromine-Radical-Mediated Selective Alkylation and Amination of Unactivated C(sp<sup>3</sup>)-H Bonds, *Chem*, 2020, **6**, 1766–1776.
- 10 P.-F. Zhong, J.-L. Tu, Y. Zhao, N. Zhong, C. Yang, L. Guo and W. Xia, Photoelectrochemical oxidative C(sp<sup>3</sup>)-H borylation of unactivated hydrocarbons, *Nat. Commun.*, 2023, **14**, 6530.
- 11 (a) C.-F. Liu, H. Wang, R. T. Martin, H. Zhao, O. Gutierrez and M. J. Koh, Olefin functionalization/isomerization enables stereoselective alkene synthesis, *Nat. Catal.*, 2021, **4**, 674–683; (b) E.-I. Negishi, G. Wang, H. Rao and Z. Xu, Alkyne Elementometalation–Pd-Catalyzed Cross-Coupling. Toward Synthesis of All Conceivable Types of Acyclic Alkenes in High Yields, Efficiently, Selectively, Economically, and Safely: “Green” Way, *J. Org. Chem.*, 2010, **75**, 3151–3182; (c) H. Jiang and A. Studer, Intermolecular radical carboamination of alkenes, *Chem. Soc. Rev.*, 2020, **49**, 1790–1811; (d) Q. Feng, Q. Wang and J. Zhu, Oxidative rearrangement of 1,1-disubstituted alkenes to ketones, *Science*, 2023, **379**, 1363–1368.
- 12 (a) S. H. Kyne, G. Lefèvre, C. Ollivier, M. Petit, V.-A. R. Cladera and L. Fensterbank, Iron and cobalt catalysis: new perspectives in synthetic radical chemistry, *Chem.*

- Soc. Rev.*, 2020, **49**, 8501–8542; (b) G. A. Filonenko, R. van Putten, E. J. M. Hensen and E. A. Pidko, Catalytic (de)hydrogenation promoted by non-precious metals – Co, Fe and Mn: recent advances in an emerging field, *Chem. Soc. Rev.*, 2018, **47**, 1459–1483; (c) Y. Liu, T. You, H.-X. Wang, Z. Tang, C.-Y. Zhou and C.-M. Che, Iron- and cobalt-catalyzed C(sp<sup>3</sup>)-H bond functionalization reactions and their application in organic synthesis, *Chem. Soc. Rev.*, 2020, **49**, 5310–5358; (d) R. Arevalo and P. J. Chirik, Enabling Two-Electron Pathways with Iron and Cobalt: From Ligand Design to Catalytic Applications, *J. Am. Chem. Soc.*, 2019, **141**, 9106–9123.
- 13 (a) J.-L. Tu, H. Gao, M. Luo, L. Zhao, C. Yang, L. Guo and W. Xia, Iron-catalyzed ring-opening of cyclic carboxylic acids enabled by photoinduced ligand-to-metal charge transfer, *Green Chem.*, 2022, **24**, 5553–5558; (b) Y. Wan, E. Ramírez, A. Ford, H. K. Zhang, J. R. Norton and G. Li, Cooperative Fe/Co-Catalyzed Remote Desaturation for the Synthesis of Unsaturated Amide Derivatives, *J. Am. Chem. Soc.*, 2024, **146**, 4985–4992.
- 14 (a) Z. Yang, D. Yang, J. Zhang, C. Tan, J. Li, S. Wang, H. Zhang, Z. Huang and A. Lei, Electrophotochemical Ce-Catalyzed Ring-Opening Functionalization of Cycloalkanols under Redox-Neutral Conditions: Scope and Mechanism, *J. Am. Chem. Soc.*, 2022, **144**, 13895–13902; (b) X.-R. Zhao, Y.-C. Zhang, Z.-W. Hou and L. Wang, Chloride-Promoted Photoelectrochemical C–H Silylation of Heteroarenes, *Chin. J. Chem.*, 2023, **41**, 2963–2968; (c) K. Yang, J. Lu, L. Li, S. Luo and N. Fu, Electrophotochemical Metal-Catalyzed Decarboxylative Coupling of Aliphatic Carboxylic Acids, *Chem. – Eur. J.*, 2022, **28**, e202202370; (d) Z. Tan, X. He, K. Xu and C. Zeng, Electrophotocatalytic C–H Functionalization of N-Heteroarenes with Unactivated Alkanes under External Oxidant-Free Conditions, *ChemSusChem*, 2022, **15**, e202102360; (e) P. Xu, P.-Y. Chen and H.-C. Xu, Scalable Photoelectrochemical Dehydrogenative Cross-Coupling of Heteroarenes with Aliphatic C–H Bonds, *Angew. Chem., Int. Ed.*, 2020, **59**, 14275–14280; (f) Z. Shen, J.-L. Tu and B. Huang, Unleashing the potentiality of metals: synergistic catalysis with light and electricity, *Org. Chem. Front.*, 2024, **11**, 4024–4040; (g) L. Wang, X. Huo, X. He, L. Ackermann and D. Wang, Photoelectrochemical nickel-catalyzed carboacylation/silanoylation of alkenes with unactivated C/Si–H bonds, *Green Chem.*, 2024, **26**, 8315–8322; (h) Y. Cao, C. Huang and Q. Lu, Photoelectrochemically driven iron-catalysed C(sp<sup>3</sup>)-H borylation of alkanes, *Nat. Synth.*, 2024, **3**, 537–544; (i) L. Zou, S. Xiang, R. Sun and Q. Lu, Selective C(sp<sup>3</sup>)-H arylation/alkylation of alkanes enabled by paired electrocatalysis, *Nat. Commun.*, 2023, **14**, 7992; (j) L. Zou, X. Zheng, X. Yi and Q. Lu, Asymmetric paired oxidative and reductive catalysis enables enantioselective alkylation of olefins with C(sp<sup>3</sup>)-H bonds, *Nat. Commun.*, 2024, **15**, 7826.
- 15 (a) J. Yu, J. Gonzalez-Cobos, F. Dappozze, P. Vernoux, A. Caravaca and C. Guillard, Basic comprehension and recent trends in photoelectrocatalytic systems, *Green Chem.*, 2024, **26**, 1682–1708; (b) P. Li, T. Zhang, M. A. Mushtaq, S. Wu, X. Xiang and D. Yan, Research Progress in Organic Synthesis by Means of Photoelectrocatalysis, *Chem. Rec.*, 2021, **21**, 841–857.
- 16 (a) S. Gao, C. Wang, J. Yang and J. Zhang, Cobalt-catalyzed enantioselective intramolecular reductive cyclization via electrochemistry, *Nat. Commun.*, 2023, **14**, 1301; (b) S. Sowmya and V. Vijaikanth, Electrochemistry and Electrocatalytic Activity of Cobaloxime Complexes, *ChemistrySelect*, 2022, **7**, e202104044; (c) E. S. Wiedner and R. M. Bullock, Electrochemical Detection of Transient Cobalt Hydride Intermediates of Electrocatalytic Hydrogen Production, *J. Am. Chem. Soc.*, 2016, **138**, 8309–8318.
- 17 (a) H. Cao, H. Jiang, H. Feng, J. M. C. Kwan, X. Liu and J. Wu, Photo-induced Decarboxylative Heck-Type Coupling of Unactivated Aliphatic Acids and Terminal Alkenes in the Absence of Sacrificial Hydrogen Acceptors, *J. Am. Chem. Soc.*, 2018, **140**, 16360–16367; (b) J.-L. Tu, J.-L. Liu, W. Tang, M. Su and F. Liu, Radical Aza-Cyclization of  $\alpha$ -Imino-oxy Acids for Synthesis of Alkene-Containing N-Heterocycles via Dual Cobaloxime and Photoredox Catalysis, *Org. Lett.*, 2020, **22**, 1222; (c) J.-L. Tu, W. Tang, S.-H. He, M. Su and F. Liu, Acceptorless dehydrogenative amination of alkenes for the synthesis of N-heterocycles, *Sci. China: Chem.*, 2022, **65**, 1330–1337; (d) J.-L. Tu, W. Tang, W. Xu and F. Liu, Iminyl-Radical-Promoted C–C Bond Cleavage/Heck-Like Coupling via Dual Cobaloxime and Photoredox Catalysis, *J. Org. Chem.*, 2021, **86**, 2929–2940; (e) J.-L. Liu, J.-L. Tu and F. Liu, Visible-Light-Promoted Intramolecular  $\alpha$ -Allylation of Aldehydes in the Absence of Sacrificial Hydrogen Acceptors, *Org. Lett.*, 2020, **22**, 7369–7372; P. Chakraborty, R. Mandal, S. Paira and B. Sundararaju, C–H bond functionalization by dual catalysis: merging of high-valent cobalt and photoredox catalysis, *Chem. Commun.*, 2021, **57**, 13075–13083; (f) M. Chen, Z.-J. Wu, J. Song and H.-C. Xu, Electrocatalytic Allylic C–H Alkylation Enabled by a Dual-Function Cobalt Catalyst, *Angew. Chem., Int. Ed.*, 2022, **61**, e202115954; (g) S. Wang, D. Ren, Z. Liu, D. Yang, P. Wang, Y. Gao, X. Qi and A. Lei, Cobalt-catalysed allylic fluoroalkylation of terpenes, *Nat. Synth.*, 2023, **2**, 1202–1210; (h) B. Sun, J. Wang, S. Zhou, J. Xu, X. Zhuang, Z. Meng, Y. Xu, Z. Zhang and C. Jin, Decatungstate/Cobalt Dual Catalyzed Dehydrogenation of Ketones Enabled by Polarity-Matched Site-Selective Activation, *ACS Catal.*, 2024, **14**, 11138–11146.